

Development of Fluidized-Bed Spray Coating  
Process for Axisymmetrical Particles

S.I. Yum and J.B. Eckenhoff  
ALZA Corporation  
Palo Alto, Calif. 94304

ABSTRACT

A technique was developed for uniform, reproducible deposition of coating materials on light-weight cylindrical particles, using the Wurster air-suspension coater. The particles used in this study had a length-to-diameter ratio of approximately four. Fluidization and coating characteristics were optimized by mixing the cylindrical particles with more symmetrical filler particle of greater density. The mixed particles produced sufficient bulk density and voidage to optimize fluidization parameters and hence uniform coating. Key variables related to the coating equipment and process were identified and

were used for process scale-up. The calculated rates of mixed-particle circulation and coating on the particles were approximately the same as experimental data obtained from three sizes of coating equipment.

### INTRODUCTION

The Wurster air-suspension coating process was introduced in 1959 as a reproducible and reliable means of encapsulating macro- and micro-size particles. The process suspends particles in a cycling air stream in which a coating material is spray-applied to the moving particles in increments each time the particles pass through the coating zone. This process, combined with in situ drying, occurs numerous times during the process, until the desired coating thickness is built up.

The Wurster coater has a relatively low maximum allowable solution injection rate and solid concentration in the solutions, and particles have to go through the coating zone a relatively larger number of times than with other coaters; as a result, coating uniformity and the reproducibility of particles processed by Wurster coaters may be superior to that produced by other equipment, particularly when a thicker coating is desired.

In this paper we generate workable fluid dynamic and mass transfer models that are predictive of the intrinsic performance characteristics of the coating equipment used for mixed particles of varying bulk density. Furthermore, we also present experimental mass transfer and fluid dynamics data for initial validation of the process and identification of the operating limits of the equipment. Three different sizes of coating equipment were used in the evaluation: 6", 12" (truncated column), and 18" air suspension coaters. The mixed-particle systems dealt with in this study consisted of different proportions of two different sizes of flat disks and cylindrical rods.

#### OPERATION OF THE WURSTER AIR-SUSPENSION COATER

The qualitative characteristics of the Wurster coater process (Figure 1) are described below.

#### REGIONS 1 AND 2

Solid particles are sucked from region 1 into region 2 because of a pressure differential that exists between the two regions: the pressure in region 2 ( $P_2$ ) is normally lower than that at region 1 ( $P_1$ ).

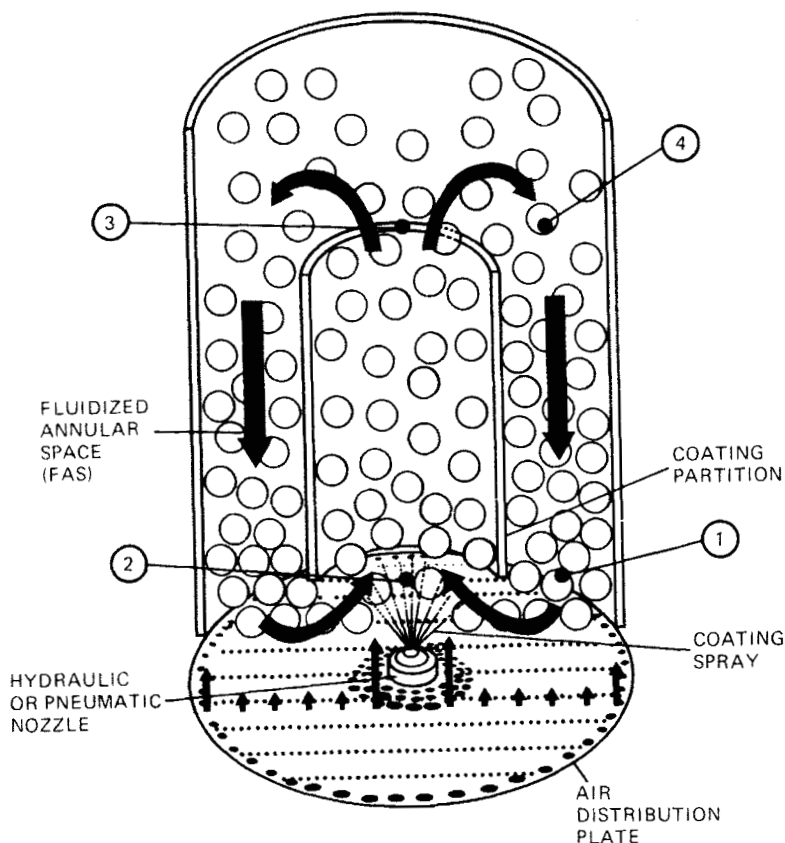


Fig. 1 - Diagram of the Wurster coating chamber.

Reverse flow of air will occur, however, if  $P_2$  is greater than  $P_1$ . This situation, which may create a sluggish flow of particles in both coating partition and fluidized annular space (FAS), occurs when the equipment is operated with too large a gap between the bottom of the partition and the air

distribution plate for a given particle size, bulk density and air flow-rate.

#### REGIONS 2 AND 3 (COATING PARTITION)

The phenomena occurring between regions 2 and 3, the coating partition, are analagous to those of a vertical pneumatic conveyor. The total air flow is the sum of the air injected through the spray nozzle, the air by-passing from region 1 to 2, and the air supplied through the openings of the air distribution plate directly under the coating partition.

Concurrent with the conveying action, liquid spray is generated from the nozzle and deposited onto the solid particles. Evaporation of volatile solvents in the liquid that is deposited on the solid particle surfaces starts in the coating partition.

Particle-particle and particle-partition interactions may lead to attrition of solid particles. The effects of collisions may vary, depending on the magnitude of kinetic energy of the particles, the specific surface area of the solid particles, the specific loading, properties of the coating material deposited on the particle surfaces, and geometric factors of the solid particles.

## REGIONS 3 AND 4 (EXPANSION CHAMBER)

The velocity of air flow begins to decrease in region 3. Between regions 3 and 4--called the expansion chamber--the air velocity decreases below that necessary to support solid particles. When the air velocity becomes less than the supporting velocity of the particles in the expansion chamber, the particles fall into region 4.

Convective drying of the solvent from the wet coating continues in the expansion chamber. Particle-particle and particle-wall interactions once again can lead to attrition in this region. Again, the effects of collisions depend on the several factors listed previously.

## REGIONS 4 AND 1 (FLUIDIZED ANNULAR SPACE)

The solid particles in this region descend, thereby forming a downward-moving fluidized bed. At steady state, the rate at which the solid particles recirculated through region 4 to region 1 is the same as that of the solid conveying rate in the coating partition or the feeding rate from region 1 to region 2.

Significant evaporation of solvent in the wet coating on the solid particles occurs between regions

4 and 1, though the rate of drying depends on voidage, air flow rate, particle geometry, and other transport properties, such as fluid density, viscosity, and diffusivity of solvent through coating.

#### EQUATIONS APPLICABLE TO THE WURSTER AIR SUSPENSION COATING PROCESS

The two-phase flow process in the partition and FAS, and the mass transfer for the coating on the particle surfaces, are assumed to be at steady state for purposes of analysis. The bed of particles in the FAS is also assumed to be minimally fluidized (i.e., the pressure drop across the height of the bed is the same as the particle weight per unit cross section of the bed). The mixed-particle system dealt with in this study consist of different proportions (both number and weight) of two different sizes of flat disks (tablets) and cylindrical rods, but average values of particle parameters were used for the analysis.

#### MIXED PARTICLE CIRCULATION RATE

For a given gap between the bottom of the partition and the air distribution plate, the solid circulation rates in the FAS and coating partition are:

$$W_1 = V_1 A_1 (1 - e_1) n_s \quad (1)$$

$$W_2 = V_2 A_2 (1 - e_2) n_s \quad (2)$$

Several empirical equations relate the above parameters. For example, Hinkle derived an empirical equation for  $V_2$  that has broad applications:

$$V_2 = V_3 (1 - 0.179 d_s^{0.3} n_s^{0.5}) \quad (3)$$

where  $d_s$  and  $n_s$  are measured in ft and lb/ft<sup>3</sup>, respectively.

Belden and Kassel derived an empirical correlation similar to Equation (3), but the equation uses the difference between  $V_3$  and  $V_2$  instead of their ratio:

$$V_3 - V_2 = 1.32 [g d_s (\frac{n_s}{n_a} - 1)]^{1/2} \quad (3a)$$

From Equations (3) and (3a), we can obtain  $V_2$  and  $V_3$  for given values of  $d_s$ ,  $n_s$ , and  $n_a$ .

Using Equations (1) and (2), we can estimate  $e_2$  at a steady state from

$$e_2 = 1 - \frac{A_1 V_1 (1 - e_1)}{A_2 V_2} \quad (4)$$

If  $A_1$ ,  $A_2$ ,  $e_1$ ,  $V_1$  and  $V_2$  are known, then  $e_2$  in Equation (4) can be calculated. Equations for  $e_1$ , and  $V_1$  are given in a later part of this section.



The number of particle recirculations between the FAS and the partition can be estimated for a given solid particle loading and circulation rate. The recycling frequency is

$$f = \frac{W_1}{W} \quad (5)$$

The total number of circulations for a given time period is then

$$N = \frac{t}{f} \quad (6)$$

Babu et al. obtained an empirical equation for the superficial air velocity at which given particulate matters begin to fluidize. Their empirical correlation can be used for an order-of-magnitude estimate of air velocity in the FAS.

$$V_4 = \frac{u_a}{n_a d_s} \{ [(25.25)^2 + 0.065 G_a]^{1/2} - 25.25 \} \quad (7)$$

$$G_a = \frac{d_s^3 n_a (n_s - n_a) g}{u_a^2} \quad (8)$$

$V_4$  can be estimated, at appropriate conditions, from the experimentally obtained values of  $d_s$  and  $n_s$ , and published data for  $u_a$  and  $n_a$ .

Yoon and Kunii derived an equation for the pressure drop in the fluidized beds by further extending the basic equations derived by Ergun. If we assume that the pressure drop in the minimally fluidized beds is approximately equal to the particle weight per unit cross sectional area of the bed, then the Yoon and Kunii equation can be rewritten as

$$\frac{L_1}{\bar{V}_b} = \frac{L_2}{g} \left[ \frac{150\mu_a (V_4 + V_1) (1 - e_1)^2}{d_s^2 y^2 e_1^2} + \frac{1.75 n_a (V_4 + V_1)^2 (1 - e_1)}{d_s y e_1} \right] \quad (9)$$

or

$$L_1 n_s (1 - e_1) = \frac{L_2}{g} \left[ \frac{150\mu_a (V_4 + V_1) (1 - e_1)^2}{d_s^2 y^2 e_1^2} + \frac{1.75 n_a (V_4 + V_1)^2 (1 - e_1)}{d_s y e_1} \right] \quad (9a)$$

A note of interest here is that  $(V_4 + V_1)$  is the slip velocity of ascending air relative to the descending solid particles, a major cause of the

pressure drop in the FAS.  $V_1$  and  $V_4$  have opposite signs; that is, if the positive direction is defined as vertical-upwards,  $V_1$  will have a negative value and  $V_4$  a positive sign.

From Equations (7) and (9) or (9a), we can estimate  $V_1$ . One key parameter required for the calculation, however, is the particle shape factor,  $y$ , which is a complex function of the geometrical factors of particles, degree of regularity of particles, particle orientation to suspending air stream, nature of air flow around the particles (laminar or turbulent), and voidage.

According to Zenz, one practical definition of  $y$  is:

$$y = \frac{0.5}{\frac{L_{\max}}{L_{\min}}} \quad (10)$$

According to Equation (10),  $y = 0.5$  for spheres.

From the superficial air velocities of  $V_3$  and  $V_4$  in Equations (3), (3a), and (7), and the cross sectional areas  $A_1$  and  $A_2$  of the equipment, we can now estimate the volumetric air flow rates:

$$Q_{a1} = V_4 A_1 \quad (11)$$

$$Q_{a2} = V_3 A_2 \quad (12)$$

# ESTIMATION OF DENSITY AND VOIDAGE OF MIXED SOLIDS PARTICLES

The approximate mean density of the mixed particle bed can be calculated from the single particle volume of each type, the number of each particle, and the mass of each particle.

$$n_s = \frac{N_1 M_1 + N_2 M_2}{N_1 \bar{V}_1 + N_2 \bar{V}_2} \quad (13)$$

The voidage in the FAS, on the other hand, is more difficult to determine. For a rough estimate, however, we can assume that the particle bed is static and then calculate the voidage from the bulk volume of the particle bed and the mean particle density. Voidage in the FAS may be approximated by Equation (14):

$$e_1 = \frac{\bar{V}_b - n_s^{-1}}{\bar{V}_b} \quad (14)$$

The bulk volume per unit mass of mixed particles can be calculated from the bulk volumes and numbers of individual particle types, or determined experimentally by measuring the total volume of the particle column, mass and volume of the single particles, and the number of particles per given particle type.

## SOLUTION COATING AND SOLVENT REMOVAL

If we assume that all of the film material applied in dilute solution is deposited on the particles without loss, then the following equation holds:

$$Q_1 C_1 = N \frac{d}{dt} (A t_m n_m) \quad (15)$$

Integration of Equation (15) between  $t = 0$  and  $t = t$  yields

$$\frac{Q_1 C_1 t}{N} = A t_m n_m \quad (16)$$

Equation (16) can be rewritten as

$$\frac{Q_1 C_1 t}{NM} = \frac{A t_m n_m}{\bar{V} n_s} = X_1 \quad (17)$$

It is interesting to note that  $X_1$  increases with  $A/\bar{V}$ .

From Equation (2) we also obtain

$$X_1 W_2 = A_2 V_2 (1 - e_2) n_s X_1 = Q_1 C_1 \quad (18)$$

Equation (18) is the weight increase of film material on the particles per unit time due to the solution injection rate  $Q_1$ , whose solid concentration is  $C_1$ .

Equation (18) can be rearranged to give

$$X_1 = \frac{Q_1 C_1}{A_2 V_2 (1 - e_2) n_s} = \frac{A t_m n_m}{\bar{V} n_s} \quad (19)$$

Equation (19) shows that  $X_1$  increases with  $A/\bar{V}$  and  $Q_1 C_1$ , but decreases as  $W_2$  ( $= W_1$  @ steady state) increases.

The cumulative weight fraction of pure solvent deposited with film material on the particles prior to evaporation can be determined from Equation (20):

$$X_2 = \frac{A t_m n_m X_3}{\bar{V} n_s} \quad (20)$$

If we assume that the solvent removal rate is controlled by diffusion in the film and by the boundary layer next to the film, the amount of solvent removed in a differential time  $\Delta t$  may be written as

$$|\Delta m| = K A \Delta C \Delta t$$

Hence, the total weight fraction of pure solvent evaporated with respect to the uncoated particles is

$$\frac{|\Delta m|}{M} = \frac{K A \Delta C \Delta t}{\bar{V} n_s} = X_4 \quad (21)$$

$X_4$  may be termed a solvent removal effectiveness

factor, which is linearly proportional to  $A/\bar{V}$ . The difference between  $X_2$  and  $X_4$  is the weight fraction of solvent left in coated particles compared to uncoated ones.  $(X_2 - X_4)$  is also linearly proportional to  $A/\bar{V}$ .

#### EXPERIMENTAL PROCEDURE

The basic data of the coating equipment and particles are listed in Tables 1 and 2. The values of the individual equipment parameters are approximate and were obtained either directly or indirectly by experiment. The composition and amounts of the mixed-particle systems are those that were found to be optimal in terms of fluidization pattern and particle attrition and agglomeration. The mixed-particle parameters are the number average values. Three mixed-particle systems were tested (i.e., one for each size of the coating equipment). The composition and relevant parameters for the three systems are given in Tables 1 and 2.

The procedure used for each experimental study was the same. The coating solution was prepared a minimum of 2 hours prior to each study in order to dissolve the coating materials and degas solutions.

TABLE 1. EQUIPMENT DESCRIPTION

	Designation (inch)		
	6	12 (truncated)	18
1. Air distribution plate			
a. area under partition (cm <sup>2</sup> )	25.3	106.9	371.2
b. are under FAS (cm <sup>2</sup> )	141.3	635.2	1185.6
c. opening area under partition (cm <sup>2</sup> )	8.3	37.4	121.7
d. opening area under FAS (cm <sup>2</sup> )	17.0	116.4	212.2
2. Diameter/Height (cm)			
a. partition	7.6/23.0	15.2/28.0	23/33
b. FAS	15/30	30/34	46/55
3. Actual loading (nominal)			
a. cylindrical particles (kg)	0.34	2.72	5.1
b. tablets (kg)	1.3 (3/8" tab)	11.0 (5/16" tab)	20.0 (5/16" tab)
c. cylindrical particles (no.)	1000	8000	15000
d. tablets (no.)	3600	44000	80000

Ten samples each of the uncoated particles were numbered and separately weighed on an analytical balance. The indicator samples were added to the mixed-particle system for determination of  $X_1$  and  $m$ .



TABLE 2. PROPERTIES OF PARTICLES

1. Density of particles* (g/cm <sup>3</sup> )	5. Mean density of mixed particles† (g/cm <sup>3</sup> )
a. = 0.7	a. = 1.20
b. = 1.4	b. = 1.13
c. = 1.3	c. = 1.13
2. Surface area and volume per particle* (cm <sup>2</sup> & cm <sup>3</sup> )	6. Bulk volume per unit weight of mixed particles† (cm <sup>3</sup> /g)
a. = 4.0 & 0.47	a. = 1.58
b. = 2.24 & 0.25	b. = 1.63
c. = 1.75 & 0.19	c. = 1.63
3. Surface area to volume ratio of particles* (cm <sup>-1</sup> )	7. Static voidage of mixed particle beds†
a. = 8.5	a. 0.47
b. = 9.0	b. 0.46
c. = 9.2	c. 0.46
4. Equivalent diameter of particles* (cm)	8. Critical dimensions of particles* (cm)
a. = 0.71	a. = 2.5 (length x 0.6 (dia.))
b. = 0.67	b. = 0.97 (dia.) x 0.46 (thick)
c. = 0.65	c. = 0.79 (dia.) x 0.46 (thick)

---

\* a. cylindrical particles (CP)  
b. 3/8" diameter tablets  
c. 5/16" diameter tablets

† a. 1000 (CP) + 3600 (3/8" tablet)  
b. 8000 (CP) + 44000 (5/16" tablets)  
c. 15000 (CP) + 80000 (5/16" tablets)

The mixed-particle systems were then fluidized and the coating solution was injected into the equipment. After injecting a predetermined volume of solution into the column, the coating process was stopped, and the indicators were reweighed for determination of  $X_1$ . Also, three samples each of the coated particles were weighed and placed in sealed vials with inert silicone septa for determination of the concentration of solvent in the coating. The mixed-particle systems, excluding those systems sampled for solvent analysis, were returned to the coating equipment along with the indicators in order to be coated with the remainder of the solution. After the entire solution had been applied to the systems, the equipment was shut down and the indicator samples reweighed for  $X_1$ . Again three samples each of the three types of particles were weighed and placed in sealed vials for determination of the solvent concentration in the coating.

Prior to each study, the gap between the bottom of the partition and the air distribution plate and the total air input rate to the coating equipment were adjusted; the time for randomly selected par-

ticles to descend the height of the FAS was also recorded.

The particular compositions of mixed-particle systems listed in Tables 1 and 2 were obtained by a trial and error. The criteria for determining the optimal composition were: 1) good fluidization patterns in the FAS and above the coating partition; 2) minimal or no particle attrition; 3) minimal or no particle-particle agglomeration; and 4) the gap between the partition and air distribution plate, the total air input to the equipment, and other process parameters were within normal operating limits.

In a separate set of tests with the three Wurster coaters, a small number of tablets of different sizes were added to the otherwise optimal mixture of cylindrical particles and regular size tablets, as described in Table 1. In these separate tests, the effects of the  $A/\bar{V}$  ratio and particle circulation rate on the rate of coating and solvent concentration in the coating were evaluated.

For all the test runs, the coating solution had a solid contents of approximately 6% (w/w); the inlet air temperature to the coating equipment was about

90°F; different sizes of atomizing liquid nozzles were used for three sizes of coaters; and the inlet air was monitored continuously with a Magnehelic® gauge.

## RESULTS AND DISCUSSION

### MIXED PARTICLE CIRCULATION RATE

Figure 2 shows the mixed-particle circulation rate for the 6" coater as a function of total air flow rate supplied to the air distribution plate. The family of lines represents the recirculation rates at the different gap settings. Similar relationships between the circulation rate and total air flow were obtained for the 12" and 18" equipment.

As the gap increased from 1" (line a) to 3" (line f), the slope of the lines increases gradually but definitely. The slopes of lines d to f are very similar while those of lines a and b are only slightly different from each other and much smaller than those of lines d to f. Therefore, the rate controlling mechanism for particle circulation may change when the gap approximates 1.5" (line c).

Figure 3 is the plot of a normalized particle circulation rate as a function of the gap at a fixed

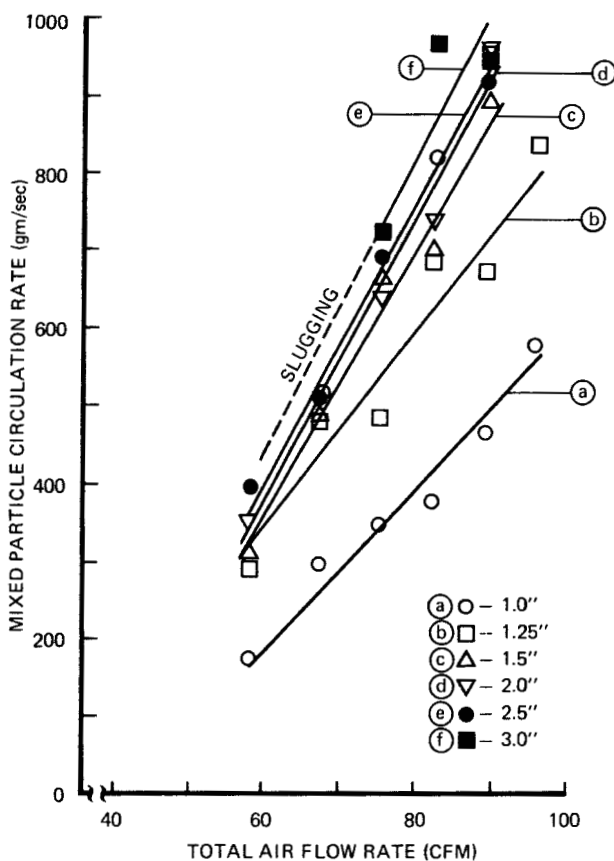


Fig. 2 - Mixed particle circulation rate in a 6" coater as a function of total air flow rate at different partition-air distributor plate distances. [Loading - as listed in Tables 1 and 2 plus 60 gm of 5/16" tablets] (Copyright 1980 ALZA Corp.)

total air input rate. At a gap of approximately 1.5", the normalized circulation rate reaches a plateau, indicating that the particle conveying through the coating partition is the rate-determining step. At

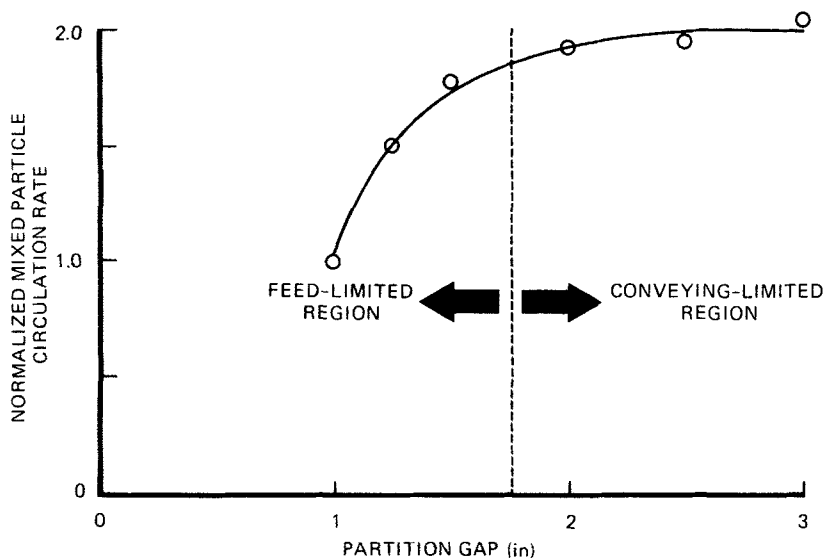


Fig. 3 - Normalized mixed-particle circulation rate as a function of partition gap. [Total air flow - 75 CFM; loading - as listed in Tables 1 and 2] (Copyright 1980 ALZA Corp.)

gaps smaller than 1.5", the particle discharge from the FAS may be the rate-controlling step. In fact, optimal fluidization and circulation patterns were achieved at gaps of approximately 1.25 to 2.0". Similar results were obtained from 12" and 18" Wurster coaters.

From Equations (1), (3), (4), (7), and (9)-(12), and the parameters of the mixed particles and the equipment listed in Tables 1 and 2, we can estimate the total air flow rate required for particle cir-

ulation and the corresponding particle circulation rates. We can also calculate the descending velocity of particles in the FAS from Equations (7) and (9), using the appropriate values of the shape factor (Equation 10 and Table 2). The calculated values (Table 3) are compared against actual data obtained experimentally. The properties of air used in the calculations were determined at 90°F.

The calculated values, though larger than the actual data, are of the same orders of magnitude. The discrepancies may be a result of 1) neglect of the by-passing air from the FAS to the coating partition; 2) under-estimate of the voidage in the FAS particle beds; 3) inaccurate estimate of the particle shape factor; or 4) over-estimate of the pressure drop in the FAS. For these calculations, no consideration was given to the effects of gap (between the partition and the air distribution plate) on the particle circulation rate and the fluid and particle velocities. We assumed that the gap size was large enough not to disturb steady state circulation of the mixed particles between the FAS and partition. As mentioned previously, we tested three mixed-particle systems and an equal

TABLE 3. COMPARISON BETWEEN ACTUAL AND CALCULATED VALUES<sup>(a,b)</sup>

	<u>Calculated</u>	<u>Actual</u>
Total air flow rate (CFM) @ 90°F and 1 atm (abs)	a. 150 b. 650 c. 1830	a. 81 b. 640 c. —
Descending velocity <sup>(c)</sup> of particles in FAS (cm/sec)	a. 10 b. 10 c. 10	a. 8 b. 3 c. 3
Particle circulation rate <sup>(d)</sup> (g/sec)	a. 900 b. 3800 c. 7100	a. 700 b. 1200 c. 2300
Coating time to obtain ( $X_1 = 0.50$ ) (hr) <sup>(e)</sup>	a. 4 b. 8 c. 10	a. 7 b. 9 c. 9
Dry coating weight at 50% weight increase ( $X_1 = 0.5$ ) (gm)	a'. 0.28 b'. 0.15 c'. 0.11	a'. 0.17 b'. 0.18 c'. 0.13
Coating Thickness at 50% weight increase ( $X_1 = 0.5$ ) (cm)	a'. 0.07 b'. 0.07 c'. 0.06	a'. 0.04 b'. 0.08 c'. 0.07

- (a) a. = 6" equipment, b. = 12" equipment, c. = 18" equipment.  
 (b) a'. = cylindrical particle, b'. = 3/8" tab., c'. = 5/16" tab.  
 (c) gap between partition and air distribution plate = 2-4"  
 (depending on equipment size).  
 (d) gap = 2-4" depending on equipment size, and at descending  
 particle speeds as indicated above.  
 (e) actual tests were done with 6% (w/w) solution, which was  
 injected at 55-400 (cm<sup>3</sup>/min) depending on equipment size.



number of equipment sizes. In order to simplify the calculations, mean values for  $d_s$ ,  $n_s$ ,  $e_1$ ,  $X$ ,  $\bar{V}_b$ , and  $L_1/L_2$  were used for all particle mixtures and equipment.

#### COATING RATE AND RESIDUAL SOLVENT

Figure 4 shows the typical fractional weight of the coating and residual solvent as a function of the cumulative volume of solution injected in a 6" coater. Both  $X_1$  and  $X_2 - X_4$  are approximately a linear

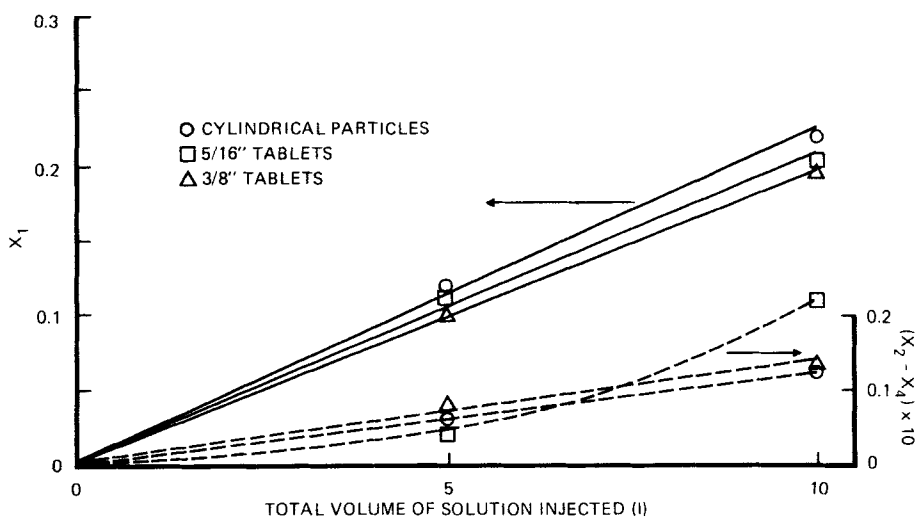


Fig. 4 - Fractional weight of coating and residual solvent as a function of solution volume injected [6% w] in a 6" coater. [Solution injection rate - 55 cc/min; partition gap - 2"; total air - 70 CFM; loading - as listed in Tables 1 and 2 plus 60 gm of 5/16" tablets] (Copyright 1980 ALZA Corp.)

function of the solution volume up to 10 liters, and are approximately proportional to the  $A/\bar{V}$  ratio of the particles. These findings are consistent with the dependence of  $X_1$  on  $Q_1$ ,  $C_1$  and  $A/\bar{V}$ , as given in Equation (19), and that of  $X_2$ - $X_4$  on  $X_3$  and  $A/\bar{V}$ , as shown in Equations (20) and (21). The values of the  $A/\bar{V}$  ratio are 8.5 ( $\text{cm}^{-1}$ ) for cylindrical particles, 9.2 for 5/16" tablets, and 9.0 for 3/8" tablets. Thus, according to predictions, all three types of particles should have approximately the same fractional gain of coating weight and fractional residual solvent level. These predictions are confirmed by the experiments (Figure 4).

As also predicted by Equations (19)-(21), both  $X_1$  and  $X_2$ - $X_4$  are inversely proportional to the particle circulation rate. In Figure 5,  $X_1$  and  $X_2$ - $X_4$  are plotted against  $W_1$  at a fixed solution injection rate and the cumulative volume of solution injected for the cylindrical particles in the 6" coater. Although both  $X_1$  and  $X_2$ - $X_4$  for the cylindrical particles decrease as  $W_1$  increases, the trends are not exactly the inverse proportionality as predicted. Similar curves were obtained for other particles and

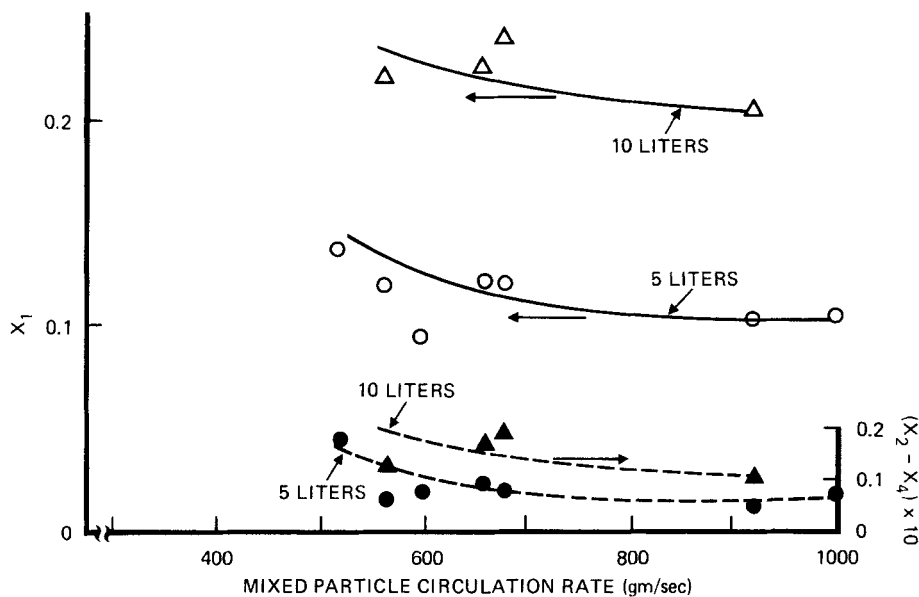


Fig. 5 - Fractional weight of coating and residual solvent as a function of mixed-particle circulation rate (cylindrical particles only) [Partition gap - 2"; solution injection rate - 55 cc/min; solution concentration - 6% w; loading - as listed in Tables 1 and 2 plus 60 gm of 5/16" tablets] (Copyright 1980 ALZA Corp.)

also from the two other Wurster coaters of larger capacities.

As mentioned previously, and shown in Figure 3, the particle circulation rate is controlled either by the discharge rate from the FAS into the partition or by the conveying rate through the partition, depending on the total air input to the coaters and the parti-

tion to the air distribution plate distance. Whenever the discharge from FAS or conveying of particles through the partition severely controlled the particle circulation, and coating solution was injected at the same time, the mixed particles usually agglomerated inside the coating partition, and hence, the coating operations had to be terminated. These kinds of problems were not observed when the discharge and conveying rates were balanced. The mixed particles in the FAS descended smoothly without significant oscillations and intermittent upward movements.

Figure 6 shows an experimentally determined region of optimal process conditions. This graph pertains to the 6" coater, but similar triangular regions were also obtained for the other coaters. The vertical side of the triangle indicates the maximum equipment capability in terms of the total air flow rate of about 90 CFM. The other two sides of the triangular region are partially due to the equipment limitations and the particle-particle agglomeration as described above. Within the optimal process window for the 6" coater, the partition gap ranges from 1.25 to 2.5" and the total air flow from

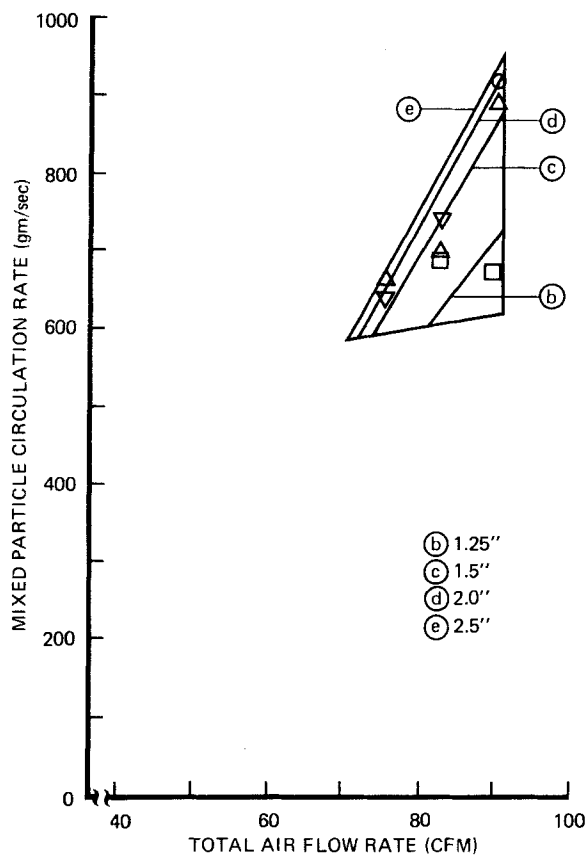


Fig. 6 - Optimal region of process conditions in the 6" coater. [Loading - as listed in Tables 1 and 2 plus 60 gm of 5/16" tablets] (Copyright 1980 ALZA Corp.)

70 to 90 CFM; the resulting particle circulation rate ranges from 600 to 950 g/sec.

The lower half of Table 3 shows the calculated and actual experimental values of the required

coating time, coating thickness, and coating weight for the situation when the coating weight is 50% of the initial particle weight. For these calculations, Equations (5), (6), and (19) were used in conjunction with relevant parameters in Tables 1 and 2.

Except for the coating thickness on the cylindrical particles and coating duration for 6" and 12" coaters, agreement between the actual and calculated values are rather good considering the rough approximations used for the equations. The relatively large discrepancies between the calculated and actual mass-transfer data for the cylindrical particles may result from the use of the same mean particle densities (Table 2) as used for the mixed-particle systems. In reality, the density of cylindrical particles is the lowest of the three particles, and hence, the calculations yield over-estimated values.

#### CONCLUSIONS

1. Light cylindrical particles of relatively large aspect ratio do not lend themselves to routine spray coating in an air-suspension coater, such as the Wurster coater. Due to the small voidage and bulk density of the particle bed, particle

circulation (conveying and fluidization) patterns are sluggish at best and usually result in intermittent bursts.

2. Addition of more symmetrical and denser particles, such as disk-like tablets, to the cylindrical particle beds yields a particle mixture that is more processable by the coating equipment. The particle circulation pattern becomes smoother, attrition of cylindrical particles is minimized, and particle-particle agglomeration is negligible compared to the pure cylindrical particle beds.
3. The above conclusions hold in the three coaters tested. An optimal ratio of tablets to cylindrical particles is approximately 4 to 1 by weight.
4. The empirical equations evaluated in this paper are useful for obtaining at least an order of magnitude estimate of total required air flow rate, particle circulation rate, and coating duration and thickness. The equations are also useful for scale-up procedures.
5. The fractional weight of residual solvent in coating is negligible compared with the fractional weight of coating on the particles. These experiments have demonstrated that in situ

drying in the coating equipment is efficient.  
Both residual solvent and coating levels are  
nearly proportional to the  $A/\bar{V}$  ratio of  
the particles.

#### NOTATION

- $A$  = surface area of particle  
 $A_1$  = cross sectional area of FAS  
 $A_2$  = cross sectional area of partition  
 $C$  = concentration of solvent in coating  
 $C_1$  = concentration of solid material in solution  
 $d_s$  = mean equivalent diameter of mixed particles  
 $e_1$  = void fraction in FAS  
 $e_2$  = void fraction in partition  
 $f$  = frequency of particle circulation  
 $g$  = gravitational acceleration  
 $G_a$  = Galileo number  
 $K$  = solvent removal rate constant for the coating  
 $L_1$  = height of FAS  
 $L_2$  = height of partition  
 $L_{\max}$  = maximum dimension of particle  
 $L_{\min}$  = minimum dimension of particle  
 $m = X_2 - X_4$ : residual solvent in coating  
 $\Delta m$  = mass of solvent evaporated



$M$  = mean mass of a single particle in mixed-particle system

$M_1$  = mass of a single particle (Type 1)

$M_2$  = mass of a single particle (Type 2)

$n_a$  = density of air

$n_m$  = density of dry membrane

$n_s$  = mean particle density

$N$  = total number of particle circulation

$N_1$  = number of particles (Type 1)

$N_2$  = number of particles (Type 2)

$Q_1$  = solution injection rate

$Q_{a1}$  = actual air flow rate into the FAS

$Q_{a2}$  = actual air flow rate into the partition

$t$  = time

$t_m$  = thickness of dry membrane

$u_a$  = viscosity of air

$V_1$  = mean particle velocity in FAS

$V_2$  = mean particle velocity in partition

$V_3$  = superficial velocity of suspending medium in partition

$V_4$  = superficial air velocity in FAS

$\bar{V}$  = volume of a particle

$\bar{V}_b$  = bulk volume of mixed particles per unit mass

$\bar{V}_1$  = volume of a particle (Type 1)

$\bar{V}_2$  = volume of a particle (Type 2)

W = total weight of mixed particles

$W_1$  = mixed particle circulation rate from FAS

$W_2$  = mixed particle circulation rate from partition

$X_1$  = weight fraction of coating with respect to the  
initial uncoated particles

$X_2$  = weight fraction of solvent deposited with  
coating

$X_3$  = weight fraction of solid material in coating  
solution

$X_4$  = solvent removal effectiveness factor

#### LITERATURE CITED

Babu, S., B. Shah, and A. Talwalker, "Fluidization Characteristics of Coal Gasification Materials," Presented at the AIChE Annual Meeting, Nov. 28 - Dec. 2 (1976).

Belden, D.H. and L.S. Kassel, "Pressure Drops Encountered in Conveying Particles of Large Diameter in Vertical Transfer Lines," Ind. Eng. Chem., 41,1174 (1949).

Ergun, S., "Fluid Flow through Packed Columns," Chem. Eng. Pr., 48,89 (1952).

- Hinkle, B.L., "Acceleration of Particles and Pressure Drops Encountered in Horizontal Pneumatic Conveying," PhD. thesis, Georgia Institute of Technology, Atlanta, Ga. (1953).
- Wurster, D.E., "Air-Suspension Technique of Coating Drug Particles: A Preliminary Report," J. Am. Pharm. Assoc. 48,451 (1959).
- Yoon, S.M. and D. Kunii, "Gas Flow and Pressure Drop through Moving Beds," Ind. Eng. PPD, 9,559 (1970).
- Zenz, F.A. and D.F. Othmer, Fluidization and Fluid-Particle Systems, Reinhold Chemical Engineering Series, Reinhold Publishing Corp., New York, p.213 (1960).